

Evidence of $\psi(3770)$ non- $D\bar{D}$ Decay to $J/\psi\pi^+\pi^-$

J. Z. Bai¹, Y. Ban⁸, J. G. Bian¹, X. Cai¹, J. F. Chang¹, H. F. Chen¹⁴, H. S. Chen¹, J. Chen⁷, J. C. Chen¹, Y. B. Chen¹, S. P. Chi¹, Y. P. Chu¹, X. Z. Cui¹, Y. M. Dai⁶, Y. S. Dai¹⁶, L. Y. Dong¹, S. X. Du¹⁵, Z. Z. Du¹, J. Fang¹, S. S. Fang¹, C. D. Fu¹, H. Y. Fu¹, L. P. Fu⁵, C. S. Gao¹, M. L. Gao¹, Y. N. Gao¹², M. Y. Gong¹, W. X. Gong¹, S. D. Gu¹, Y. N. Guo¹, Y. Q. Guo¹, Z. J. Guo¹³, S. W. Han¹, F. A. Harris¹³, J. He¹, K. L. He¹, M. He⁹, X. He¹, Y. K. Heng¹, T. Hong¹, H. M. Hu¹, T. Hu¹, G. S. Huang¹, L. Huang⁵, X. P. Huang¹, X. B. Ji¹, C. H. Jiang¹, X. S. Jiang¹, D. P. Jin¹, S. Jin¹, Y. Jin¹, Z. J. Ke¹, Y. F. Lai¹, F. Li¹, G. Li¹, H. H. Li⁴, J. Li¹, J. C. Li¹, K. Li⁵, Q. J. Li¹, R. B. Li¹, R. Y. Li¹, W. Li¹, W. G. Li¹, X. Q. Li⁷, X. S. Li¹², C. F. Liu¹⁵, C. X. Liu¹, Fang Liu¹⁴, F. Liu⁴, H. M. Liu¹, J. B. Liu¹, J. P. Liu¹⁵, R. G. Liu¹, Y. Liu¹, Z. A. Liu¹, Z. X. Liu¹, G. R. Lu³, F. Lu¹, H. J. Lu¹⁴, J. G. Lu¹, Z. J. Lu¹, X. L. Luo¹, E. C. Ma¹, F. C. Ma⁶, J. M. Ma¹, L. L. Ma⁹, Z. P. Mao¹, X. C. Meng¹, X. H. Mo², J. Nie¹, Z. D. Nie¹, S. L. Olsen¹³, H. P. Peng¹⁴, N. D. Qi¹, C. D. Qian¹⁰, J. F. Qiu¹, G. Rong¹, D. L. Shen¹, H. Shen¹, X. Y. Shen¹, H. Y. Sheng¹, F. Shi¹, L. W. Song¹, H. S. Sun¹, S. S. Sun¹⁴, Y. Z. Sun¹, Z. J. Sun¹, S. Q. Tang¹, X. Tang¹, D. Tian¹, Y. R. Tian¹², G. L. Tong¹, G. S. Varner¹³, J. Wang¹, J. Z. Wang¹, L. Wang¹, L. S. Wang¹, M. Wang¹, Meng Wang¹, P. Wang¹, P. L. Wang¹, W. F. Wang¹, Y. F. Wang¹, Zhe Wang¹, Z. Wang¹, Zheng Wang¹, Z. Y. Wang², C. L. Wei¹, N. Wu¹, X. M. Xia¹, X. X. Xie¹, G. F. Xu¹, Y. Xu¹, S. T. Xue¹, M. L. Yan¹⁴, W. B. Yan¹, G. A. Yang¹, H. X. Yang¹², J. Yang¹⁴, S. D. Yang¹, M. H. Ye², Y. X. Ye¹⁴, J. Ying⁸, C. S. Yu¹, G. W. Yu¹, J. M. Yuan¹, Y. Yuan¹, Q. Yue¹, S. L. Zang¹, Y. Zeng⁵, B. X. Zhang¹, B. Y. Zhang¹, C. C. Zhang¹, D. H. Zhang¹, H. Y. Zhang¹, J. Zhang¹, J. M. Zhang³, J. W. Zhang¹, L. S. Zhang¹, Q. J. Zhang¹, S. Q. Zhang¹, X. Y. Zhang⁹, Y. J. Zhang⁸, Yiyun Zhang¹¹, Y. Y. Zhang¹, Z. P. Zhang¹⁴, D. X. Zhao¹, Jiawei Zhao¹⁴, J. W. Zhao¹, P. P. Zhao¹, W. R. Zhao¹, Y. B. Zhao¹, Z. G. Zhao^{1*}, J. P. Zheng¹, L. S. Zheng¹, Z. P. Zheng¹, X. C. Zhong¹, B. Q. Zhou¹, G. M. Zhou¹, L. Zhou¹, N. F. Zhou¹, K. J. Zhu¹, Q. M. Zhu¹, Yingchun Zhu¹, Y. C. Zhu¹, Y. S. Zhu¹, Z. A. Zhu¹, B. A. Zhuang¹, B. S. Zou¹.

(BES Collaboration)

¹ Institute of High Energy Physics, Beijing 100039, People's Republic of China

² China Center of Advanced Science and Technology, Beijing 100080, People's Republic of China

³ Henan Normal University, Xinxiang 453002, People's Republic of China

⁴ Huazhong Normal University, Wuhan 430079, People's Republic of China

⁵ Hunan University, Changsha 410082, People's Republic of China

⁶ Liaoning University, Shenyang 110036, People's Republic of China

⁷ Nankai University, Tianjin 300071, People's Republic of China

⁸ Peking University, Beijing 100871, People's Republic of China

⁹ Shandong University, Jinan 250100, People's Republic of China

¹⁰ Shanghai Jiaotong University, Shanghai 200030, People's Republic of China

¹¹ Sichuan University, Chengdu 610064, People's Republic of China

¹² Tsinghua University, Beijing 100084, People's Republic of China

¹³ University of Hawaii, Honolulu, Hawaii 96822

¹⁴ University of Science and Technology of China, Hefei 230026, People's Republic of China

¹⁵ Wuhan University, Wuhan 430072, People's Republic of China

¹⁶ Zhejiang University, Hangzhou 310028, People's Republic of China

* Visiting professor to University of Michigan, Ann Arbor, MI 48109 USA

Evidence of $\psi(3770)$ decays to a non- $D\bar{D}$ final state is observed. A total of $11.8 \pm 4.8 \pm 1.3$ $\psi(3770) \rightarrow J/\psi\pi^+\pi^-$ events are obtained from a data sample of 27.7 pb^{-1} taken at center-of-mass energies around 3.773 GeV using the BES-II detector at the BEPC. The branching fraction is determined to be $BF(\psi(3770) \rightarrow J/\psi\pi^+\pi^-) = (0.34 \pm 0.14 \pm 0.09)\%$, corresponding to the partial width of $\Gamma(\psi(3770) \rightarrow J/\psi\pi^+\pi^-) = (80 \pm 33 \pm 23) \text{ keV}$.

PACS numbers:

I. INTRODUCTION

The $\psi(3770)$ resonance is believed to be a mixture of the 1^3D_1 and 2^3S_1 states of the $c\bar{c}$ system [1]. Since its mass is above the open charm-pair threshold and its width is two orders of magnitude larger than that of the $\psi(2S)$, it is thought to decay almost entirely to

pure $D\bar{D}$ [2]. However, Lipkin pointed out that the $\psi(3770)$ could decay to non- $D\bar{D}$ final states with a large branching fraction [3]. There are theoretical calculations [4, 5, 6, 7] that estimate the partial width for $\Gamma(\psi(3770) \rightarrow J/\psi\pi^+\pi^-)$ based on the multipole expansion in QCD. Recently Kuang [7] used the Chen-Kuang potential model to obtain a partial width for

$\psi(3770) \rightarrow J/\psi\pi\pi$ in the range from 37 to 170 keV, corresponding to 25 to 113 keV for $\psi(3770) \rightarrow J/\psi\pi^+\pi^-$ from isospin symmetry. In this paper, we report evidence for $\psi(3770) \rightarrow J/\psi\pi^+\pi^-$ based on a data sample of 27.7 pb^{-1} taken in the center-of-mass (c.m.) energy region from 3.738 GeV to 3.885 GeV using the upgraded Beijing spectrometer (BES-II) at the Beijing Electron Positron Collider (BEPC).

II. THE BES-II DETECTOR

The BES-II is a conventional cylindrical magnetic detector that is described in detail in Ref. [8]. A 12-layer Vertex Chamber (VC) surrounding the beryllium beam pipe provides input to the event trigger, as well as coordinate information. A forty-layer main drift chamber (MDC) located just outside the VC yields precise measurements of charged particle trajectories with a solid angle coverage of 85% of 4π ; it also provides ionization energy loss (dE/dx) measurements which are used for particle identification. Momentum resolution of $1.7\%\sqrt{1+p^2}$ (p in GeV/c) and dE/dx resolution of 8.5% for Bhabha scattering electrons are obtained for the data taken at $\sqrt{s} = 3.773 \text{ GeV}$. An array of 48 scintillation counters surrounding the MDC measures the time of flight (TOF) of charged particles with a resolution of about 180 ps for electrons. Outside the TOF, a 12 radiation length, lead-gas barrel shower counter (BSC), operating in limited streamer mode, measures the energies of electrons and photons over 80% of the total solid angle with an energy resolution of $\sigma_E/E = 0.22/\sqrt{E}$ (E in GeV) and spatial resolutions of $\sigma_\phi = 7.9 \text{ mrad}$ and $\sigma_Z = 2.3 \text{ cm}$ for electrons. A solenoidal magnet outside the BSC provides a 0.4 T magnetic field in the central tracking region of the detector. Three double-layer muon counters instrument the magnet flux return and serve to identify muons with momentum greater than 500 MeV/c. They cover 68% of the total solid angle.

III. DATA ANALYSIS

A. Monte Carlo simulation

To understand the main source of background in the study of the decay $\psi(3770) \rightarrow J/\psi\pi^+\pi^-$, we developed a Monte Carlo generator. The Monte Carlo simulation includes the initial state radiation (ISR) at one loop order, in which the actual center-of-mass energies after ISR are generated according to Ref. [9]. The $\psi(2S)$ and $\psi(3770)$ are generated using energy dependent Breit-Wigner functions according to Eq.(38.53) of Ref. [10] in which the ratio of $\Gamma_{el}(s)/\Gamma_{tot}(s) = \Gamma_{\psi(2S) \rightarrow e^+e^-}/\Gamma_{tot}$ and the branching fraction of $\psi(2S) \rightarrow J/\psi\pi^+\pi^-$ in the formula are assumed to be constant. The beam energy spread ($\sigma_{E_{beam}} = 1.37 \text{ MeV}$) is taken into account in the simulation. Since there is no unique description

and solution for the low energy $\pi\pi$ production amplitude [11], the correction of the decay rate due to the $\pi\pi$ production amplitude is neglected in the making of the event generator. However the effect of the variations in the correction to the decay rate on the estimated number of $\psi(2S) \rightarrow J/\psi\pi^+\pi^-$ is considered in the final background subtraction in subsection E. Fig. 1 shows the distribution of $J/\psi\pi^+\pi^-$ events with $J/\psi \rightarrow l^+l^-$ ($l = e$ or μ) as a function of the actual energy remaining after initial state photon radiation, which is determined by our Monte Carlo generator, where the branching fraction for $\psi(3770) \rightarrow J/\psi\pi^+\pi^-$ is set to be 0.35%, while the branching fractions for $\psi(2S) \rightarrow J/\psi\pi^+\pi^-$ and $J/\psi \rightarrow l^+l^-$ are taken from the Particle Data Group (PDG) [10].

There are two peaks which are around 3.686 GeV and 3.773 GeV in Fig. 1, where the $J/\psi\pi^+\pi^-$ events from the $\psi(2S)$ decay are given by the dotted histogram, while the events from the $\psi(3770)$ decay are given by the solid histogram. There are two components in the higher mass peak. One is from $\psi(3770)$ production, and the another is from $\psi(2S)$ production which is due to the tail of $\psi(2S)$ Breit-Wigner function. This type of $\psi(2S)$ production (called type B of $\psi(2S)$ in this Letter) is indicated by the dotted histogram around 3.773 GeV. The $J/\psi\pi^+\pi^-$ events in the lower mass peak are produced around the peak of the $\psi(2S)$ Breit-Wigner function (called type A of $\psi(2S)$ in this Letter), and are due to ISR energy return to the $\psi(2S)$ peak. The "type B" of $\psi(2S)$ is the main source of background events in the experimental study of the decay $\psi(3770) \rightarrow J/\psi\pi^+\pi^-$. This background event has the same topology as that as the decay of $\psi(3770) \rightarrow J/\psi\pi^+\pi^-$. To get the number of $\psi(3770) \rightarrow J/\psi\pi^+\pi^-$ signal events, the number of the background events of $\psi(2S) \rightarrow J/\psi\pi^+\pi^-$ has to be subtracted from the observed candidate events of $J/\psi\pi^+\pi^-$ based on analyzing the Monte Carlo events.

In the energy region from 3.738 to 3.885 GeV in Fig. 1, there are 1724 $\psi(3770) \rightarrow J/\psi\pi^+\pi^-$ events and 747 $\psi(2S) \rightarrow J/\psi\pi^+\pi^-$ events. The generated events as shown in Fig. 1 are put through the full detector simulation based on the GEANT simulation package. The fully simulated events are used for study of the main background.

B. Events selection

To search for the decay of $\psi(3770) \rightarrow J/\psi\pi^+\pi^-$, $J/\psi \rightarrow e^+e^-$ or $\mu^+\mu^-$, $\mu^+\mu^-\pi^+\pi^-$ and $e^+e^-\pi^+\pi^-$ candidate events are selected. These are required to have four charged tracks with zero total charge. Each track is required to have a good helix fit, to be consistent with originating from the primary event vertex, and to satisfy $|\cos\theta| < 0.85$, where θ is the polar angle.

Pions and leptons must satisfy particle identification requirements. For pions, the combined confidence level (CL), calculated for the π hypothesis using the dE/dx

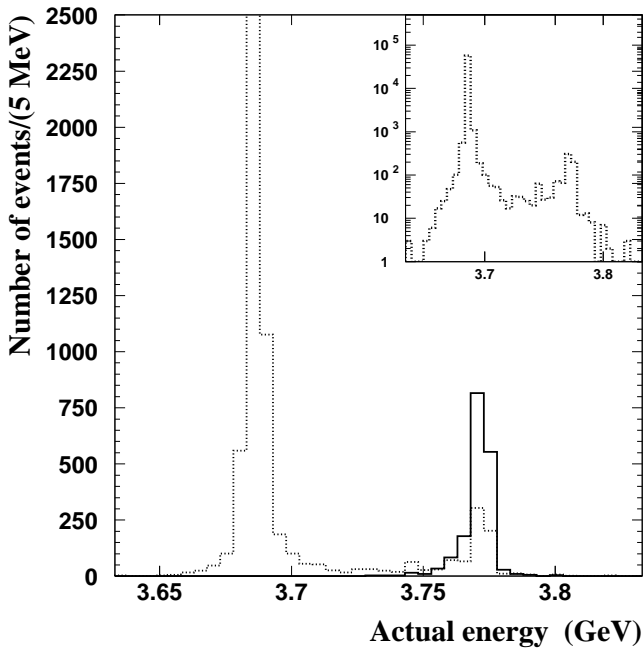


FIG. 1: The numbers of $\psi(3770) \rightarrow J/\psi\pi^+\pi^-$ (solid line) and $\psi(2S) \rightarrow J/\psi\pi^+\pi^-$ (dotted line) as a function of the actual energy remaining after ISR, where J/ψ is set to decay to l^+l^- ; the events are generated with the Monte Carlo generator at the c.m. energies at which the data were collected from 3.738 to 3.885 GeV. The insert on the right-top shows the distribution of the energy at which $\psi(2S) \rightarrow J/\psi\pi^+\pi^-$ events are produced.

and TOF measurements, is required to be greater than 0.1%. In order to reduce γ conversion background, in which the e^+ and e^- from a converted γ are misidentified as π^+ and π^- , an opening angle cut, $\theta_{\pi^+\pi^-} > 20^\circ$, is imposed. For electron identification, the combined confidence level, calculated for the e hypothesis using the dE/dx , TOF and BSC measurements, is required to be greater than 1%, and the ratio $CL_e/(CL_e+CL_\mu+CL_\pi+CL_K)$ is required to be greater than 0.7. If a charged track hits the muon counter, and the z and $r\phi$ positions of the hit match with the extrapolated positions of the reconstructed MDC track, the charged track is identified as a muon.

The candidate events of $e^+e^-\pi^+\pi^-$ or $\mu^+\mu^-\pi^+\pi^-$ satisfying the above selection criteria are further analyzed by using two different analysis methods to be discussed in subsection C and subsection D.

C. Analysis of the $\pi^+\pi^-$ recoil mass

The mass recoiling against the $\pi^+\pi^-$ system is calculated using

$$M_{\text{REC}}(\pi^+\pi^-) = \sqrt{(E_{cm} - E_{\pi^+\pi^-})^2 - |\vec{P}_{\pi^+\pi^-}|^2},$$

where E_{cm} is the c.m. energy, $E_{\pi^+\pi^-}$ and $\vec{P}_{\pi^+\pi^-}$ are the total energy and momentum of the $\pi^+\pi^-$ system, respectively.

Fig. 2 shows the distribution of the masses recoiling against the $\pi^+\pi^-$ system for candidate events with total energy within $\pm 2.5\sigma_{E_{\pi^+\pi^-l^+l^-}}$ of the nominal c.m. energy at which the events were obtained and with a dilepton invariant mass within ± 150 MeV of the J/ψ mass, where $\sigma_{E_{\pi^+\pi^-l^+l^-}}$ is the standard deviation of the distribution of the energy of the $\pi^+\pi^-l^+l^-$. Two peaks are observed. The higher one is from the "type A" of $\psi(2S)$ events produced by radiative return to the peak of the $\psi(2S)$, while the small enhancement around 3.1 GeV is mostly from $\psi(3770)$ decays, but also contains the contamination of the "type B" of $\psi(2S)$ decays. This is confirmed by analyzing the Monte Carlo sample generated with the Monte Carlo generator as mentioned before. Fig. 3 shows the same distribution from analysis of the Monte Carlo events for $\psi(2S)$ and $\psi(3770)$ production and decays to $J/\psi\pi^+\pi^-$ with $J/\psi \rightarrow l^+l^-$ final states. The Monte Carlo events are generated at the c.m. energies at which the data were collected. The size of the Monte Carlo sample is twenty times larger than the data. There are also two peaks; the higher one is from the "type A" of $\psi(2S)$ events; the small enhancement around 3.1 GeV consist of two components. One is from the "type B" of $\psi(2S)$ event production and decays as shown by the solid line histogram; the other one is from $\psi(3770)$ production and decays which come from the events as shown by the solid histogram in Fig.1. The error bars in Fig. 3 are based on the total number of observed events of $\psi(3770) \rightarrow J/\psi\pi^+\pi^-$ and $\psi(2S) \rightarrow J/\psi\pi^+\pi^-$. The differences between the error bars and the histogram as shown around 3.1 GeV correspond to $\psi(3770)$ production and decay to $J/\psi\pi^+\pi^-$.

Monte Carlo studies show that the distributions of the masses recoiling from the $\pi^+\pi^-$ system for the "type A" of $\psi(2S)$ events can be described by two Gaussian functions. One Gaussian function is for the "type A" of $\psi(2S)$ production from the events for which the nominal c.m. energy is set at 3.773 GeV, and the other one is from the events for which the nominal c.m. energies are set off 3.773 GeV. Using triple Gaussian functions, one of which describes the peak near the J/ψ mass and two of which represent the second and the third peaks of the events from the "type A" of $\psi(2S)$, and a first order polynomial to represent the background to fit the mass distributions as shown by the solid histograms for both the data (Fig. 2) and the Monte Carlo (Fig. 3) sample, we obtain a total of 25.5 ± 5.9 $J/\psi \rightarrow l^+l^-$ signal events from both the $\psi(3770) \rightarrow J/\psi\pi^+\pi^-$ and the "type B" of $\psi(2S) \rightarrow J/\psi\pi^+\pi^-$ events and 220.5 ± 26.0 "type B" of $\psi(2S) \rightarrow J/\psi\pi^+\pi^-$ events, respectively. The curves give the best fits to the data and the Monte Carlo sample. The fitted peak positions and standard deviations of the Gaussian functions used for the fits in Fig. 2 and Fig. 3 are listed in Table I.

TABLE I: Summary of the fitted results of the data and the Monte Carlo sample in Fig. 2 and Fig. 3.

Figure	Peak	Mass [MeV]	σ_M [MeV]
	Peak1	3097.8 ± 3.0	9.9 ± 2.4
2	Peak2	3182.4 ± 1.8	23.3 ± 2.8
	Peak3	3182.5 ± 0.6	7.6 ± 0.7
	Peak1	3099.4 ± 1.3	13.1 ± 2.9
3	Peak2	3180.8 ± 0.4	22.4 ± 0.7
	Peak3	3185.0 ± 0.2	7.4 ± 0.2

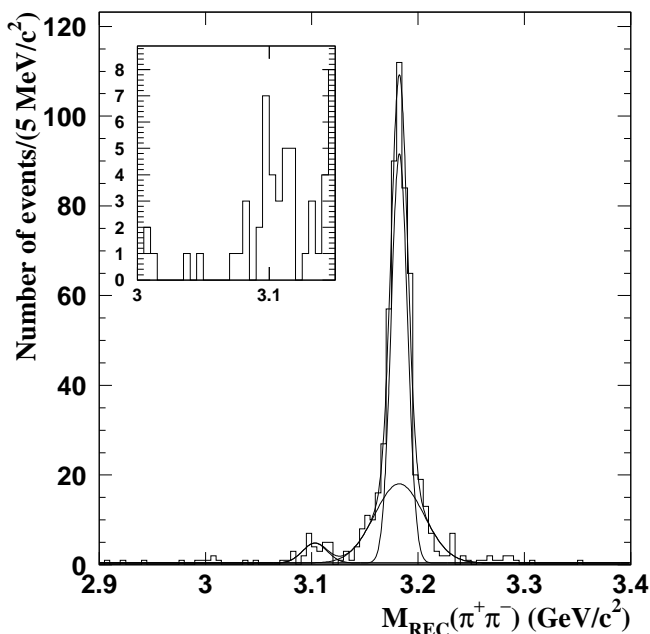


FIG. 2: The distribution of the masses recoiling from the $\pi^+\pi^-$ system for $l^+l^-\pi^+\pi^-$ events; the insert on the left-top shows the mass distribution in a local region around 3.1 GeV; the curves give the best fit to the recoil mass spectrum. see text.

D. Kinematic fit

In order to reduce background and improve momentum resolution, candidate events are subjected to four-constraint kinematic fits to either the $e^+e^- \rightarrow \mu^+\mu^-\pi^+\pi^-$ or the $e^+e^- \rightarrow e^+e^-\pi^+\pi^-$ hypothesis. Events with a confidence level greater than 1% are accepted. Fig. 4 shows the dilepton masses determined from the fitted lepton momenta of the accepted events. There are clearly two peaks. The lower mass peak is mostly due to $\psi(3770) \rightarrow J/\psi\pi^+\pi^-$, while the higher one is due to the "type A" of $\psi(2S) \rightarrow J/\psi\pi^+\pi^-$. Since the higher mass peak is produced by the radiative return to the $\psi(2S)$ peak, its energy will be approximately 3.686 GeV, while the c.m. energy is set to the nominal

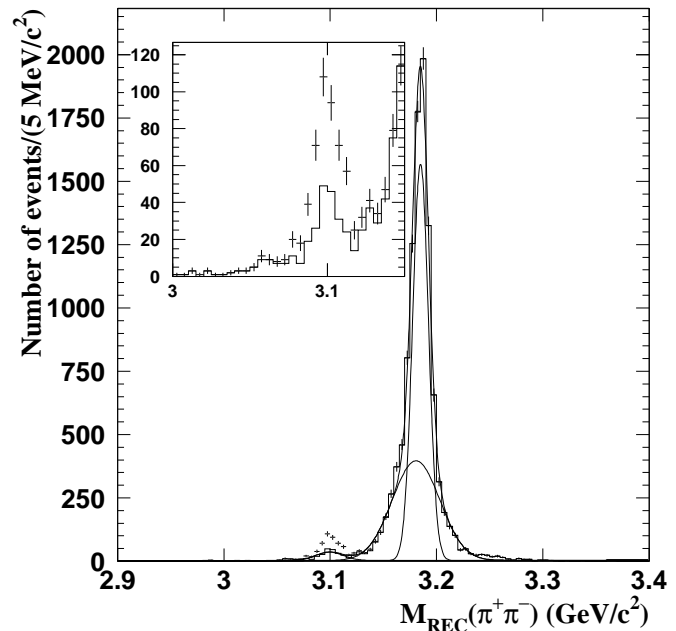


FIG. 3: The distribution of the masses recoiling from $\pi^+\pi^-$ for the Monte Carlo events of $\psi(2S) \rightarrow J/\psi\pi^+\pi^-$ and $\psi(3770) \rightarrow J/\psi\pi^+\pi^-$ with $J/\psi \rightarrow l^+l^-$; these events are generated with the Monte Carlo generator; where the error bars represent the sum total of the two components, while the histogram is for the $\psi(2S) \rightarrow J/\psi\pi^+\pi^-$ from both the "type A" and "type B" of $\psi(2S)$; the curves give the best fits to the recoil mass spectrum from the Monte Carlo $\psi(2S) \rightarrow J/\psi\pi^+\pi^-$ events only; the insert on the left-top shows the mass distribution in a local region around 3.1 GeV; here two components from the $\psi(3770) \rightarrow J/\psi\pi^+\pi^-$ and the "type B" of $\psi(2S) \rightarrow J/\psi\pi^+\pi^-$ are clearly seen.

energy in the kinematic fitting. Therefore, the dilepton masses calculated based on the fitted lepton momenta from $\psi(2S) \rightarrow J/\psi\pi^+\pi^-$, $J/\psi \rightarrow l^+l^-$ are shifted upward to about 3.18 GeV.

A maximum likelihood fit to the mass distribution in Fig. 4, using three Gaussian functions to describe the mass distribution of the $l^+l^-\pi^+\pi^+$ combinations and a first order polynomial to represent the broad background as used to fit the $\pi^+\pi^-$ recoil mass distributions in Fig. 2 and Fig. 3, yields a J/ψ mass value of 3097.8 ± 3.0 MeV and a signal of 17.8 ± 4.8 $J/\psi \rightarrow l^+l^-$ events. The curves give the best fit to the data.

As discussed in Section C, there is a contribution from the "type B" of $\psi(2S) \rightarrow J/\psi\pi^+\pi^-$ that can pass the event selection criteria and can lead to an accumulation of the recoil masses of the $\pi^+\pi^-$ and/or the fitted dilepton masses around 3.097 GeV. This is the main source of background to $\psi(3770) \rightarrow J/\psi\pi^+\pi^-$. Fig. 5 shows the distribution of the fitted dilepton masses of the Monte Carlo events of $\psi(3770) \rightarrow J/\psi\pi^+\pi^-$ and $\psi(2S) \rightarrow J/\psi\pi^+\pi^-$ with $J/\psi \rightarrow l^+l^-$ as shown in Fig. 1. Here the histogram shows the dilepton mass distribution for

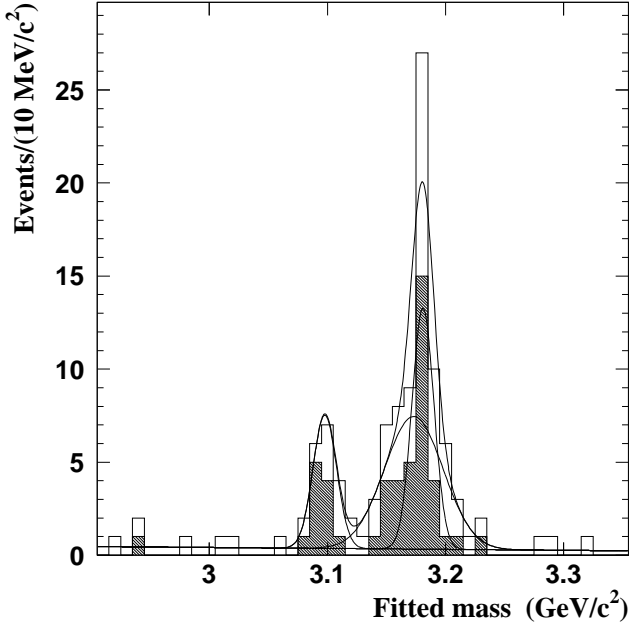


FIG. 4: The distribution of the fitted dilepton masses for the events of $l^+l^-\pi^+\pi^-$ from the data; the hatched histogram is for $\mu^+\mu^-\pi^+\pi^-$, while the open one is for $e^+e^-\pi^+\pi^-$; the curves give the best fit to the data.

$\psi(2S) \rightarrow J/\psi\pi^+\pi^-$ only. The higher mass peak is due to the "type A" of $\psi(2S) \rightarrow J/\psi\pi^+\pi^-$ events, and the lower one is from the "type B" of $\psi(2S) \rightarrow J/\psi\pi^+\pi^-$ events. The error bars show the sum total of the observed events of $\psi(2S) \rightarrow J/\psi\pi^+\pi^-$ and $\psi(3770) \rightarrow J/\psi\pi^+\pi^-$. The differences between the error bars and the histogram correspond to the observed events of $\psi(3770) \rightarrow J/\psi\pi^+\pi^-$. Fitting the mass distribution for the $\psi(2S)$ events only (histogram) with the same triple Gaussian functions as mentioned before yields 119 ± 12.1 J/ψ events from the "type B" of $\psi(2S) \rightarrow J/\psi\pi^+\pi^-$ decays.

E. Other background and background subtraction

1. Other background

Some physics processes, such as two-photon events, $e^+e^- \rightarrow e^+e^-\mu^+\mu^-$ (where the slow muons are misidentified as pions) and $e^+e^- \rightarrow e^+e^-\pi^+\pi^-$, $e^+e^- \rightarrow \tau^+\tau^-$ and $e^+e^- \rightarrow D\bar{D}$ could be sources of background.

To check if there are some background contaminations in the observed $J/\psi\pi^+\pi^-$ events due to the possible sources of background, we generated 1×10^5 two-photon Monte Carlo events (which is about 4 times larger than the data), 6×10^5 $e^+e^- \rightarrow \text{hadrons}$ Monte Carlo events (which is about 1.6 times larger than the data), and 2.3×10^6 $e^+e^- \rightarrow D\bar{D}$ Monte Carlo events (which is about 13 times larger than the data), where the D

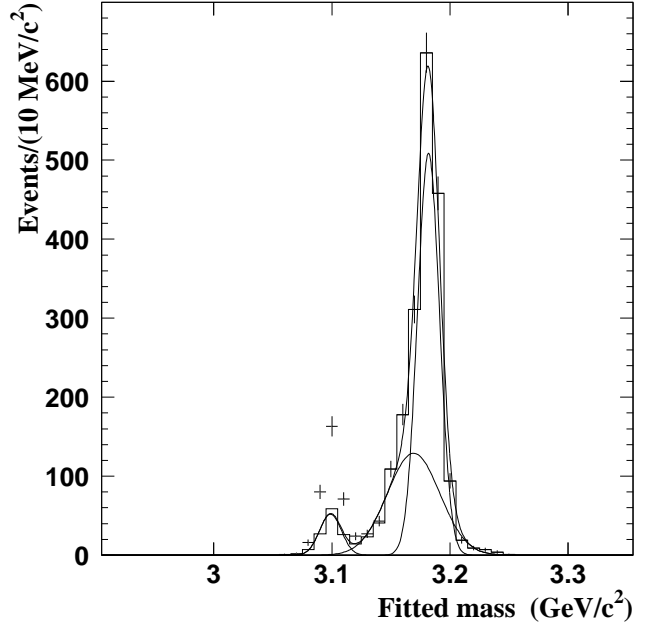


FIG. 5: The distribution of the fitted dilepton masses for the events of $l^+l^-\pi^+\pi^-$ from the Monte Carlo sample of $\psi(3770) \rightarrow J/\psi\pi^+\pi^-$ and $\psi(2S) \rightarrow J/\psi\pi^+\pi^-$ which are generated with the Monte Carlo generator (see section A); the histogram is for $\psi(2S) \rightarrow J/\psi\pi^+\pi^-$, while the error bars are the sum of $\psi(3770) \rightarrow J/\psi\pi^+\pi^-$ and $\psi(2S) \rightarrow J/\psi\pi^+\pi^-$, where the J/ψ is set to decay to l^+l^- .

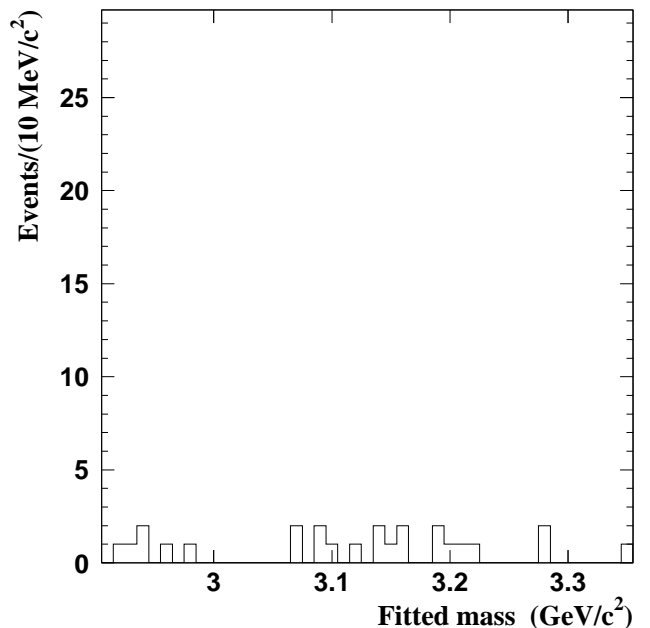


FIG. 6: The distributions of the dilepton masses of the events of $l^+l^-\pi^+\pi^-$ from the data taken at 4.03 GeV with the BES-I at the BEPC.

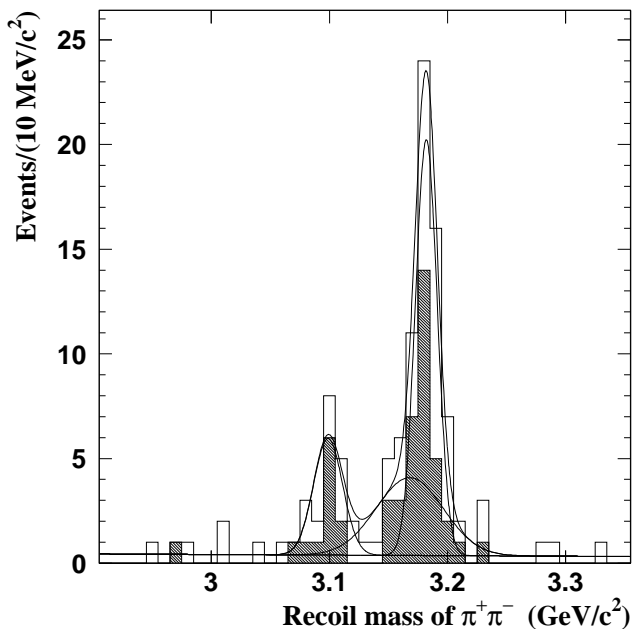


FIG. 7: The distribution of the masses recoiling against the $\pi^+\pi^-$ system calculated using the measured momenta for events that pass the kinematic fit requirement, where the hatched histogram is for events of $\mu^+\mu^-\pi^+\pi^-$ and the open one is for $e^+e^-\pi^+\pi^-$.

and \bar{D} mesons are set to decay to all possible final states according to the decay modes and branching fractions quoted from PDG [10]. These Monte Carlo events are fully simulated with the GEANT-based simulation package. None of the simulated possible background events were misidentified as $J/\psi\pi^+\pi^-$ events.

The candidate $J/\psi\pi^+\pi^-$ events could also be produced in the continuum process, such as $e^+e^- \rightarrow l^+l^-\pi^+\pi^-$ and $e^+e^- \rightarrow \tau^+\tau^-$, and satisfy the selection criteria. From analyzing a sample of 6.6 pb^{-1} taken at 3.65 GeV with the BES-II detector, a sample of 5.1 pb^{-1} taken in the energy region from 3.544 to 3.600 GeV and a sample of 22.3 pb^{-1} taken at 4.03 GeV with the BES-I detector, no significant $J/\psi\pi^+\pi^-$, $J/\psi \rightarrow l^+l^-$ events are observed. Fig. 6 shows the distribution of the fitted dilepton masses of the events of $l^+l^-\pi^+\pi^-$ which satisfy the selection criteria; these events are from the data taken with the BES-I detector at 4.03 GeV. The distribution of the fitted dilepton masses is flat, which is consistent with the background distribution. Hence the continuum background is negligible.

2. Number of background

After normalizing to the total luminosity of the data set, we estimate that there are $11.0 \pm 1.3 \pm 2.4$ background events from the "type B" of $\psi(2S) \rightarrow J/\psi\pi^+\pi^-$

in the 25.5 ± 5.9 $J/\psi \rightarrow l^+l^-$ signal events obtained by fitting to the $\pi^+\pi^-$ recoil mass distribution of Fig. 2 and $6.0 \pm 0.5 \pm 1.3$ background events from the "type B" of $\psi(2S) \rightarrow J/\psi\pi^+\pi^-$ in the 17.8 ± 4.8 $J/\psi \rightarrow l^+l^-$ signal events obtained by fitting to the fitted dilepton mass distribution of Fig. 4, where the first errors are statistical and the second are systematic. The later arise from the uncertainties (± 1.1) and (± 0.6) in the $\psi(2S)$ resonance parameters and the uncertainties (± 2.2) and (± 1.2) coming from the ambiguities of the knowledge of the low energy $\pi\pi$ production amplitude in $\psi(2S) \rightarrow J/\psi\pi^+\pi^-$. The two terms correspond to the uncertainty on the production amplitude predicted by different theoretical models [11] for analyzing the $\pi^+\pi^-$ recoil mass spectrum and the fitted dilepton mass spectrum, respectively. The theoretical models are based on the PCAC and current algebra or chiral perturbative theory predictions in which the various $\pi^+\pi^-$ rescattering corrections are taken into account to get better unitarity behavior at higher energy.

F. Number of signal events $\psi(3770) \rightarrow J/\psi\pi^+\pi^-$

The probability that the 17.8 events observed are due to a fluctuation of the $6.0 \pm 0.5 \pm 1.3$ events is 1.1×10^{-3} . After subtracting the numbers of the background events, $14.5 \pm 6.4 \pm 2.4$ and $11.8 \pm 4.8 \pm 1.3$ signal events of $\psi(3770) \rightarrow J/\psi\pi^+\pi^-$ are retained from analyzing the recoil masses of $\pi^+\pi^-$ (see Fig. 2) and the fitted dilepton masses (see Fig. 4) of the events $l^+l^-\pi^+\pi^-$, respectively.

In this analysis, the possible interference between the $\psi(2S)$ background and the $\psi(3770)$ signal is neglected since the decay wave functions of $\psi(3770)$ and $\psi(2S)$ are orthogonal [6]. The BES detector is symmetric enough in the spatial direction and there is no bias for the event selections about the momentum direction of the particles. Therefore the interference terms cancel after integrating over the pion momenta.

To test whether there is any bias in the kinematic fit, we examine the $\pi^+\pi^-$ recoil mass distribution for the events passing the kinematic fit requirements. Fig. 7 shows the recoil mass distribution, where the recoil masses are calculated as mentioned in Section C, but the events are not required to satisfy the total energy cut and dilepton invariant mass cut. There are also two peaks, similar to those in Fig. 4, observed clearly. Fitting to the mass spectrum with the same functions as described above yields a J/ψ mass value of 3100.1 ± 3.8 MeV and a signal of 17.2 ± 5.0 events, consistent with the 17.8 ± 4.8 signal events obtained by fitting to the dilepton mass distribution in Fig. 4.

Table II summarizes the fitted peak positions and standard deviations of the Gaussian functions used for the fits in Fig. 4, Fig. 5 and Fig. 7.

TABLE II: Summary of the fitted results of the data and Monte Carlo sample in Fig. 4, Fig. 5 and Fig. 7.

Figure	Peak	Mass [MeV]	σ_M [MeV]
	Peak1	3097.8 ± 3.0	9.9 ± 2.4
Fig. 4	Peak2	3173.1 ± 5.5	24.8 ± 5.7
	Peak3	3180.9 ± 2.4	9.3 (fixed)
	Peak1	3098.8 ± 0.7	9.1 ± 0.5
Fig. 5	Peak2	3169.2 ± 0.7	22.2 ± 0.5
	Peak3	3181.8 ± 0.2	9.3 (fixed)
	Peak1	3100.1 ± 3.8	13.2 ± 3.5
Fig. 7	Peak2	3177.1 ± 3.9	19.6 (fixed)
	Peak3	3185.4 (fixed)	7.0 (fixed)

G. The number of $\psi(3770)$ produced

The total number of $\psi(3770)$ events is obtained from our measured luminosities at each c.m. energy and from calculated cross sections for $\psi(3770)$ production at these energies. The Born level cross section at energy E is given by

$$\sigma_{\psi(3770)}^B(E) = \frac{12\pi\Gamma_{ee}\Gamma_{\text{tot}}(E)}{(E^2 - M^2)^2 + M^2\Gamma_{\text{tot}}^2(E)},$$

where the $\psi(3770)$ resonance parameters, Γ_{ee} and M , are taken from the PDG [10] and $\Gamma_{\text{tot}}(E)$ is chosen to be energy dependent and normalized to the total width Γ_{tot} at the peak of the resonance [10][12][13]. In order to obtain the observed cross section, it is necessary to correct for ISR. The observed $\psi(3770)$ cross section, $\sigma_{\psi(3770)}^{\text{obs}}(s_{\text{nom}})$, is reduced by a factor $g(s_{\text{nom}}) = \sigma_{\psi(3770)}^{\text{obs}}(s_{\text{nom}})/\sigma_{\psi(3770)}^B(s_{\text{nom}})$, where s_{nom} is the c.m. energy squared and $\sigma_{\psi(3770)}^B(s_{\text{nom}})$ is the Born cross section. The ISR correction for $\psi(3770)$ production is calculated using a Breit-Wigner function and the radiative photon energy spectrum [9][13]. With the calculated cross sections for $\psi(3770)$ production at each energy point around 3.773 GeV and the corresponding luminosities, the total number of $\psi(3770)$ events in the data sample is determined to be $N_{\psi(3770)}^{\text{prod}} = (1.85 \pm 0.37) \times 10^5$, where the error is mainly due to the uncertainty in the observed cross section for $\psi(3770)$ production.

IV. RESULT

A. Monte Carlo efficiency

The efficiencies for reconstruction of the events of $\psi(3770) \rightarrow J/\psi\pi^+\pi^-$ with $J/\psi \rightarrow e^+e^-$ and $J/\psi \rightarrow \mu^+\mu^-$ are estimated by Monte Carlo simulation. Monte Carlo study shows that the efficiencies are $\epsilon_{\psi(3770) \rightarrow J/\psi\pi^+\pi^-, J/\psi \rightarrow e^+e^-} = 0.146 \pm 0.003$ and

$\epsilon_{\psi(3770) \rightarrow J/\psi\pi^+\pi^-, J/\psi \rightarrow \mu^+\mu^-} = 0.174 \pm 0.003$, where the errors are statistical. These give the averaged efficiency for detection of $J/\psi \rightarrow e^+e^-$ and $J/\psi \rightarrow \mu^+\mu^-$ events to be $\epsilon_{\psi(3770) \rightarrow J/\psi\pi^+\pi^-, J/\psi \rightarrow l^+l^-} = 0.160 \pm 0.002$.

B. Branching fraction and partial width

Using these numbers and the known branching fractions for $J/\psi \rightarrow e^+e^-$ and $\mu^+\mu^-$ [10], the branching fraction for the non- $D\bar{D}$ decay $\psi(3770) \rightarrow J/\psi\pi^+\pi^-$ is measured to be

$$BF(\psi(3770) \rightarrow J/\psi\pi^+\pi^-) = (0.338 \pm 0.143 \pm 0.086)\%,$$

where the first error is statistical and the second systematic arising from the uncertainties in the total number of $\psi(3770)$ produced (20%), tracking efficiency (2.0% per track), particle identification (2.2%), background shape (6%), $\psi(2S) \rightarrow J/\psi\pi^+\pi^-$ background subtraction (12%) and the averaged branching fraction for $J/\psi \rightarrow l^+l^-$ (1.2%). Adding these uncertainties in quadrature yields the total systematic error of 25.5%.

Using Γ_{tot} from the PDG [10], this branching fraction corresponds to a partial width of

$$\Gamma(\psi(3770) \rightarrow J/\psi\pi^+\pi^-) = (80 \pm 33 \pm 23) \text{ keV},$$

where the first error is statistical and the second systematic. The systematic uncertainty in the measured partial width arises from the systematic uncertainty in the measured branching fraction (25.5%) and the uncertainty in the total width of $\psi(3770)$ (11.5%) [10].

As a consistency check, we can use the number of signal events $\psi(3770) \rightarrow J/\psi\pi^+\pi^-$ obtained from analyzing the recoil masses of the $\pi^+\pi^-$ from the events $l^+l^-\pi^+\pi^-$ to calculate the branching fraction. The detection efficiency is $\epsilon_{\psi(3770) \rightarrow J/\psi\pi^+\pi^-, J/\psi \rightarrow l^+l^-} = 0.194$. These numbers yield a branching fraction $BF(\psi(3770) \rightarrow J/\psi\pi^+\pi^-) = (0.342 \pm 0.142 \pm 0.097)\%$, which is in good agreement with the value obtained above, indicating that the kinematic fit result is reliable.

V. SUMMARY

In summary, the branching fraction for $\psi(3770) \rightarrow J/\psi\pi^+\pi^-$ has been measured. From a total of $(1.85 \pm 0.37) \times 10^5$ $\psi(3770)$ events, $11.8 \pm 4.8 \pm 1.3$ non- $D\bar{D}$ decays of $\psi(3770) \rightarrow J/\psi\pi^+\pi^-$ events are observed, leading to a branching fraction of $BF(\psi(3770) \rightarrow J/\psi\pi^+\pi^-) = (0.34 \pm 0.14 \pm 0.09)\%$, and a partial width $\Gamma(\psi(3770) \rightarrow J/\psi\pi^+\pi^-) = (80 \pm 33 \pm 23) \text{ keV}$.

ACKNOWLEDGEMENTS

We would like to thank the BEPC staff for their strong efforts and the members of the IHEP computing center for their helpful assistance. We acknowledge Professor Yu-Ping Kuang and Professor Kuang-Ta Chao for many helpful discussions on the non- DD decay of $\psi(3770)$. This work is supported in part by the National Natural Science Foundation of China under contracts Nos.

19991480, 10225524, 10225525, the Chinese Academy of Sciences under contract No. KJ 95T-03, the 100 Talents Program of CAS under Contract Nos. U-24, U-25, and the Knowledge Innovation Project of CAS under Contract Nos. U-602, U-34(IHEP); by the National Natural Science Foundation of China under Contract No. 10175060(USTC); and by the Department of Energy under Contract No. DE-FG03-94ER40833 (U Hawaii).

-
- [1] P.A. Rapidis *et al.*, MARK-I Collaboration, Phys. Rev. Lett. **39** (1978) 526.
- [2] W. Bacino *et al.*, DELCO Collaboration, Phys. Rev. Lett. **40** (1978) 671.
- [3] H.J. Lipkin, Phys. Lett. **B179** (1986) 278.
- [4] K. Lane, Harvard Report No. HUTP-86/A045, (1986).
- [5] Y.P. Kuang and T.M. Yan, Phys. Rev. **D24** (1981) 2874.
- [6] Y.P. Kuang and T.M. Yan, Phys. Rev. **D41** (1990) 155.
- [7] Y.P. Kuang, Phys. Rev. **D65** (2002) 094024.
- [8] J.Z. Bai *et al.*, BES Collaboration, Nucl. Instr. Meth. **A458** (2001) 627.
- [9] E.A. Kuraev and V.S. Fadin, Sov. J. Nucl. Phys. **41** (1985) 466.
- [10] S. Eidelman *et al.*, Particle Data Group, Phys. Lett. **B 592** (2004) 1.
- [11] Robert L. Goble and Jonathan L. Rosner, Phys. Rev. **D5** (1972) 2345; H.Q. Zheng *et al.*, Nucl. Phys. **A733** (2004) 235; Lowell S. Brown, Phys. Rev. Lett. **35** (1975) 1.
- [12] R.H. Schindler *et al.*, Phys. Rev. **D21** (1980) 2716.
- [13] M. Ablikim *et al.*, BES Collaboration, arXiv:hep-ex/0411013, Phys. Lett. **B 603** (2004) 130.